Supporting Information

Physical Vapor Deposition of Cyanine Dyes and First Application in Organic Electronic Devices

Donatas Gesevičius,[a,e] Antonia Neels[b], Léo Duchêne[c], Erwin Hack,[d] Jakob Heier[a,] and Frank Nüesch[a,f]*

a. Laboratory for Functional Polymers, Swiss Federal Laboratories for Materials Science and Technology, Empa, Überlandstrasse 129, Dübendorf, Switzerland
b. Center for X-ray Analytics, Swiss Federal Laboratories for Materials Science and Technology, Empa, Überlandstrasse 129, Dübendorf, Switzerland
c. Laboratory Materials for Energy Conversion, Swiss Federal Laboratories for Materials Science and Technology, Empa, Überlandstrasse 129, Dübendorf, Switzerland
d. Laboratory for Transport at Nanoscale Interfaces, Swiss Federal Laboratories for Materials Science and Technology, Empa, Überlandstrasse 129, Dübendorf, Switzerland
e. Institute of Chemical Sciences and Engineering, ISIC, Ecole Polytechnique Fédérale de Lausanne, EPFL, Station 6, CH-1015 Lausanne, Switzerland
f. Institut des Matériaux, Ecole Polytechnique Fédérale de Lausanne, EPFL, Station 6, CH-1015 Lausanne, Switzerland
E-mail: jakob.heier@empa.ch

Table of Contents

General Information

General Notation for this Work

- Two symmetrical indolenine derivatives connected with a trimethine chain

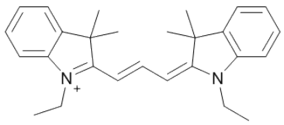

1-Ethyl-2-[3-(1-ethyl-1,3-dihydro-3,3-dimethyl-2*H*-indol-2-ylidene)-1-propen-1-yl]-3,3-dimethyl-3H-indolium (Cy3)

- Weakly coordinating anion

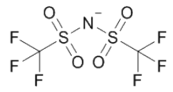

Bis((trifluoromethyl)sulfonyl)imide (TFSI)

- Abbreviation for the dye used in this work

Cy3TFSI

Figure S1. Overview of the notation of the compound used for this work.

Anion Exchange Procedure

The detailed background and experimental setup for the ion exchange procedure can be found in literature.[1]

Synthesis of Cy3TFSI

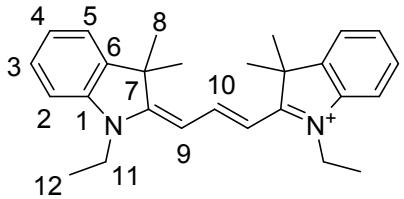

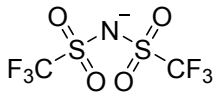

0.5 g of Cy3I solved in 250 mL MeCN were passed through 1.3 g of the anion exchange resin loaded with the bistriflylimide. After evaporation of the solvent and drying for 24 h at 9.3x10^{-3} mbar a shiny red solid was obtained. Yield: quantitative.

For X-Ray analysis suitable crystals were obtained by slowly cooling of a saturated ethanol solution.

[$C_{29}H_{33}F_6N_3O_4S_2$] 665.71 g mol^{-1}

^{1}H NMR (400 MHz, Chloroform-*d*) δ: 8.41 (t, J = 13.5 Hz, 1H), 7.50 – 7.32 (m, 4H), 7.27 (t, J = 7.5 Hz, 3H), 7.14 (d, J = 7.9 Hz, 2H), 6.53 (d, J = 13.4 Hz, 2H), 4.18 (q, J = 7.3 Hz, 4H), 1.73 (s, 12H), 1.45 (t, J = 7.2 Hz, 6H), 1.37 (t, J = 7.3 Hz, 1H) ppm.

^{13}C NMR (101 MHz, Chloroform-d) δ: 173.8 (C9), 150.9 (C11), 141.7 (C1), 140.8 (C6), 129.1 (C3), 125.7 (C4), 122.4 (C5), 120.1 (q, J = 321 Hz, (CF_3)), 110.9 (C2), 103.0 (C10), 49.4 (C7), 39.7 (C12), 28.1 (C8), 12.4 (C13) ppm.

^{19}F NMR (377 MHz, Chloroform-*d*) δ: -78.65 ppm.

Elemental analysis: Calculated: [C] 52.32, [H] 5.00, [N] 6.31, [F] 17.12 [S] 9.63.

Found: [C] 52.44, [H] 5.14, [N] 6.34, [F] 17.25 [S] 9.67.

Thin Film Evaporation

Qualitative trials of Cy3TFSI evaporation

Figure S2. Visual results of the evaporated Cy3TFSI films on glass, ITO/TiO_2 ITO/MoO_3 and ITO/PEDOT:PSS substrates (left to right).

UV-Vis absorbance

To determine the molar extinction coefficient 1.44×10^{-4} mol L^{-1} acetonitrile stock solution of the Cy3TFSI compound was prepared. Subsequently solutions with five different concentrations were prepared by diluting the stock solution (**Table S1**).

Table S1. Used concentrations for the generation of calibration points in UV-Vis.

Solution	Concentration (mol L^{-1})
	Cy3TFSI
1	1.70 x 10^{-8}
2	6.35 x 10^{-8}
3	5.85 x 10^{-7}
4	6.85 x 10^{-7}
5	2.39 x 10^{-6}

All measurements were performed in a 1 cm quartz glass cuvette using 99.8 % acetonitrile as reference for the baseline. The relative molar extinction coefficient was calculated by extracting the slope of the resulting plot of concentration against absorbance intensity.

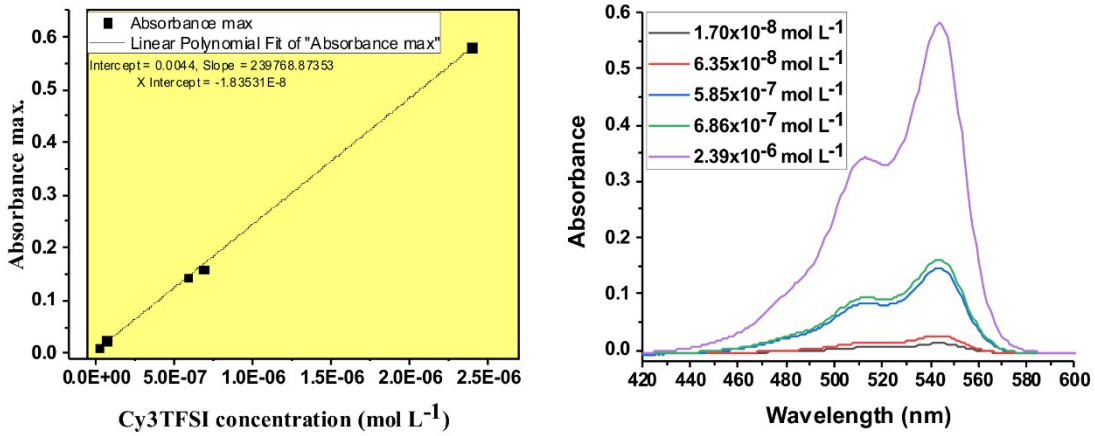

Figure S3. Concentration dependent absorbance and linear fit of the absorbance maxima against concentration.

The extracted optical data are summarized in **Table S2**. The optical band gap was calculated from the onset of the absorbance at higher wavelengths with the following equation.

$$E_{g(onset)} = \frac{h \times c}{\lambda_{onset}}$$

λ_{onset}: Onset of absorption band at higher wavelength, h: Planck constant, c: speed of light.

The oscillator strength describes the probability of a transition from a lower to an upper energy state. The higher the value the easier the electrons can be excited and the stronger absorbing is the dye.

$$f = 4.319 \times 10^{-9} \int \varepsilon(\upsilon)\, d\upsilon$$

$\varepsilon(\upsilon)$: Molar extinction coefficient as a function of wavenumber, υ: Wavenumber.

The peak in **Figure S3** was assumed to represent the full band of the lowest energy π-π^* transition and was integrated to calculate the oscillator strength.

First, the wavelength (given in nm) was converted into wavenumbers with the following formula:

$$\upsilon = 1/(\lambda * 10^{-7})$$

Then the extinction coefficient was calculated for each wavenumber with the following formula:

$$\varepsilon_{(\upsilon)} = A/(c * d)$$

c: concentration in mol·L^{-1}, d: thickness of cuvette in cm, A: absorbance.

The calculations were performed for each recorded data point of the spectra.

Table S2. Calculated data from recorded UV-Vis spectra. * Onset energy at higher wavelengths obtained from MeCN solution.

Compound	ε_{max} (L mol^{-1} cm^{-1})	λ_{max} (nm)	λ_{onset} (nm)	$E_{(onset)*}$ (eV)	f
Cy3TFSI	2.40×10^5	544	565	2.19	1.87

Cyclic Voltammetry for Estimation of HOMO/LUMO Energy Levels

Cyclic voltammetry (CV) measurements were performed on a PGStat 30 potentiostat (Autolab) using a three cell electrode system (Au working electrode, Pt counter electrode and an Ag/AgCl reference electrode). Two electrolyte solutions of tetrabutylammonium perchlorate and tetrabutylammonium chloride were prepared in DMF each 0.1 mol/L. Each

measurement needs 50 ml of tetrabutylammonium perchlorate (25 mL account for the measurement and 25 mL for cleaning) and 10 mL of tetrabutylammonium chloride (4 mL for measurement and 6 mL for cleaning) solutions. The following amount of the Cy3TFSI was used (**Table S3**).

Table S3. Weighted quantities of the dyes.

Dye	m (mg)	n (mol)
Cy3TFSI	10.0	1.50×10^{-5}

The Ferrocene solution was prepared qualitatively by adding a spatula of ferrocene in 10 mL of electrolyte solution. All potentials were referenced to NHE by adopting a potential of +0.72 V vs. NHE for Fc/Fc+ in DMF.[4] The rotating disk was equilibrated before first measurement for 30 min at 3000 rpm. Then the rotation speed was reduced to 50 rpm and was kept constant for all measurements. Before each measurement step the solution was fumigated with argon for 15 min. The solvent window was determined by running 30 cycles from -1.5 V until 1.5 V with a scanning rate of 2 V/s, subsequently the scanning rate was reduced to 0.1 V/s and the baseline curve was recorded. Then the Cy3TFSI was added to the solution and the above described measurement procedure was repeated. The negative potential window was adjusted to -0.75 V.

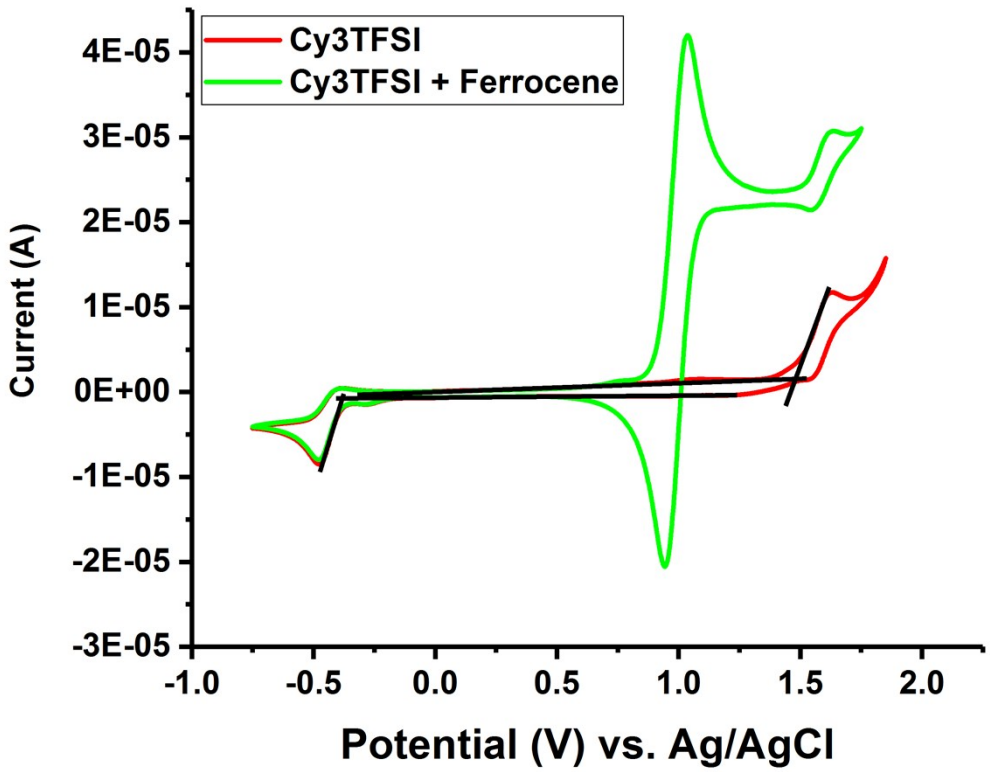

Figure S4. Cyclic voltammetry curves of Cy3TFSI.

The calculations of the $E_{g(el)}$ (HOMO/LUMO gap) are based on the assumption that a positive cathodic current can be referred to a reduction process, a negative anodic current to an oxidation process. Therefore the oxidation potential corresponds to electron extraction from the HOMO level, while the reduction potential is associated with the electron affinity and indicates the LUMO level. By analysing the recorded spectra graphically it is possible to determine the respective reduction $E_{red(dye)}^{onset}$ or oxidation $E_{ox(dye)}^{onset}$ onset potentials. It is notable that the recorded cyclic voltammograms are showing irreversible processes for all investigated dyes, so that the intersection onset of the corresponding peak has to be chosen as the respective potential. While for the ferrocene which undergoes a reversible process the potential is calculated according to:

$$E_{1/2(Ferrocene)}^{ox} = \frac{E_{pc}^{ox} + E_{pa}^{ox}}{2}$$

$E_{1/2(Ferrocene)}^{ox}$: half-curve potential, E_{pa}^{ox}: anodic peak potential, E_{pc}^{ox} : cathodic peak potential.

The potentials were measured against an Ag/AgCl reference. The used conversion constant for ferrocene in DMF is 0.72 V.[4] The correction value against NHE for ferrocene was calculated as follows:

$$\text{Korr.}_{\text{Ferrocene}} = 0.72 - E_{1/2(Ferrocene)}^{ox}$$

To calculate the corrected values for the onset potentials against NHE potential the following assumptions were made:

$$E_{ox(dye)\ vs.\ NHE}^{onset} = E_{ox(dye)}^{onset} + Korr._{Ferrocene}$$
$$E_{red(dye)\ vs.\ NHE}^{onset} = E_{red(dye)}^{onset} + Korr._{Ferrocene}$$

The calculation of the HOMO and LUMO was performed by using empirical equations.[5] The used onset potentials were corrected against NHE as described above.

$$E_{HOMO} = -\left(E_{ox(dye)\ vs.\ NHE}^{onset} + 4.5\right)eV$$
$$E_{LUMO} = -\left(E_{red(dye)\ vs.\ NHE}^{onset} + 4.5\right)eV$$
$$E_{g(el)} = E_{HOMO} - E_{LUMO}$$

Table S4. Calculated data from the CV measurement.

Substance	$E_{ox(dye)}^{onset}$ **/V**	$E_{red(dye)}^{onset}$**/V**	$E_{\frac{1}{2}ox(FeCp_2)}^{0}$**/V**	E_{HOMO}**/eV**	E_{LUMO}**/eV**	$E_{g(el)}$**/eV**
Cy3TFSI	1.48	-0.38	0.99	-5.71	-3.85	1.86

Thermal Behaviour of Cy3I and Cy3TFSI

The dynamic TGA for both materials was carried out with a heating cycle from room temperature to 600°C followed by a cooling to room temperature with dynamic steps of 10°C min^{-1}.

The aluminium crucible was sealed and contained five holes in the lid.

Temperature Program for isothermal TGA measurement for both components:

All dynamic steps were carried out at 10°C min^{-1} under constant nitrogen or helium flow respectively.

Dynamic: heating to 100°C; Isothermal: 100°C, 30 min; Dynamic: heating to 200°C; Isothermal: 200°C, 30 min; Dynamic: heating to 220°C; Isothermal: 220°C, 30 min; Dynamic: 230 °C; Isothermal: 230°C, 30 min; Dynamic: heating to 240°C; Isothermal: 240°C, 30 min; Dynamic: heating to 250°C; Isothermal: 250°C, 30 min; Dynamic: heating to 260°C; Isothermal: 260°C, 30 min; Dynamic: heating to 270°C; Isothermal: 270°C, 30 min; Dynamic: heating to 280°C; Isothermal: 280°C, 30 min; Cooling to room temperature.

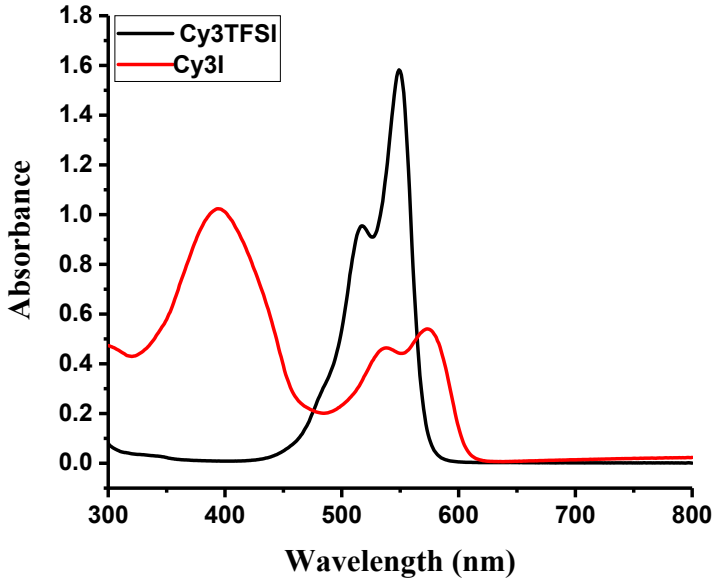

Figure S5. Qualitative UV-Vis spectra in ethanol solution rinsed from the substrate of evaporated starting material (Cy3I) and Cy3TFSI.

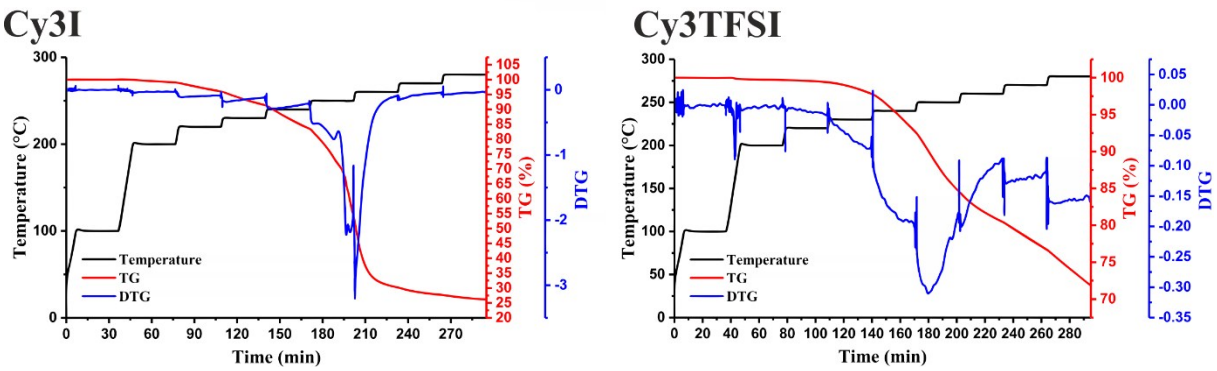

Figure S6. Isothermal TGA of both components with relative mass loss.

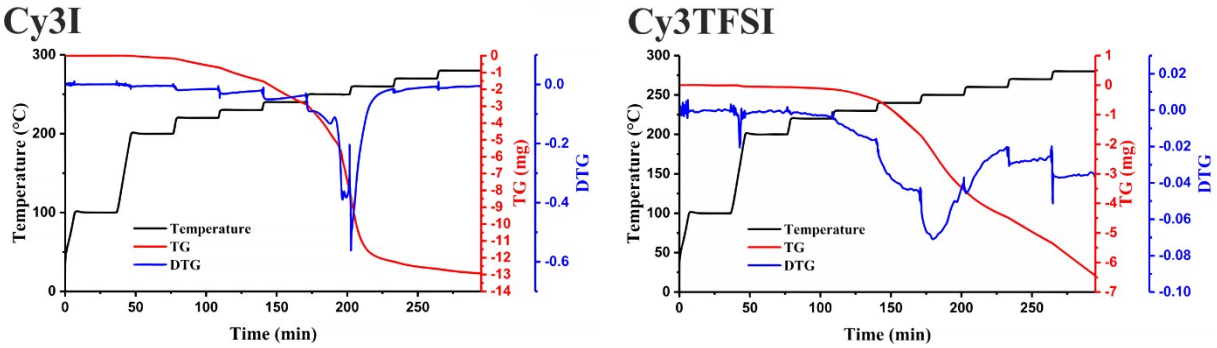

Figure S7. Isothermal TGA of both components with absolute mass loss.

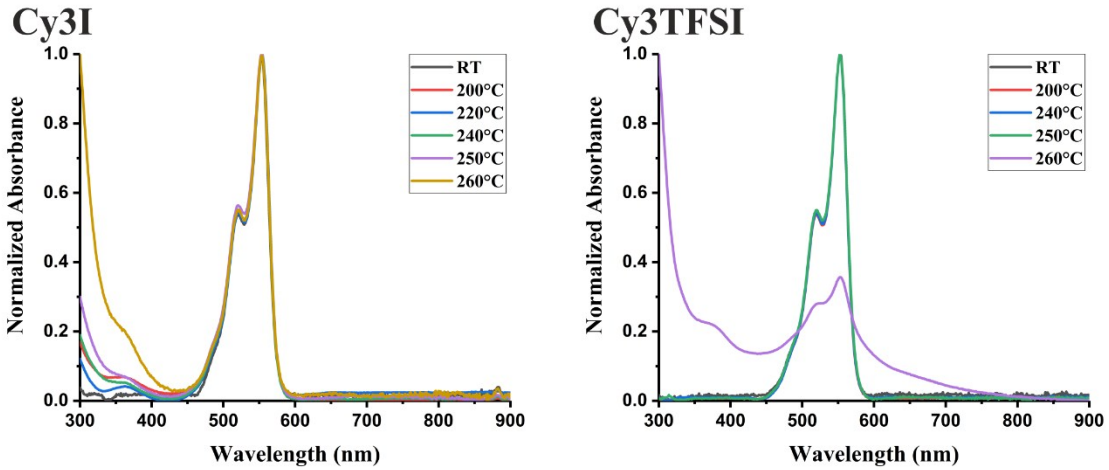

Figure S8. Normalized UV-Vis spectra of heated residual material from TGA crucibles at certain temperatures.

The mass loss of each isothermal section was extracted and plotted against the time of each isothermal step. Subsequently the slopes of the linear fit were extracted and plotted against temperature.

Table S5. Cy3I extracted slope of (dm/dt) vs. t and coefficient of determination at a certain temperature.

T/°C	Slope	R^2
200	0.0052	0.99
220	0.01701	0.99
230	0.0263	0.99
240	0.04573	0.99
250	0.14865	0.92
260	0.09757	0.77
270	0.01349	0.97
280	0.00851	0.98

Table S6. Cy3TFSI extracted slope of (dm/dt) vs. t and coefficient of determination at a certain temperature.

T/°C	Slope	R^2
200	0.00083	0.97
220	0.00232	0.98
230	0.01196	0.99
240	0.03963	0.99
250	0.06227	0.99
260	0.02901	0.99
270	0.02770	0.99
280	0.03601	0.99

Table S7. Calculated values for Cy3TFSI in 220-250°C range to determine the enthalpy of vaporization.

T/K	T^{-1}/K^{-1}	10^5 (-dm/dt)/g min^{-1}	$ln[T^{1/2}$ (-dm/dt)]
493.15	0.00203	1.70	-7.8813
503.15	0.00199	2.63	-7.4355
513.15	0.00195	4.57	-6.87247
523.15	0.00191	1.49	-5.68398
slope	-18379.8		
R^2	0.94		

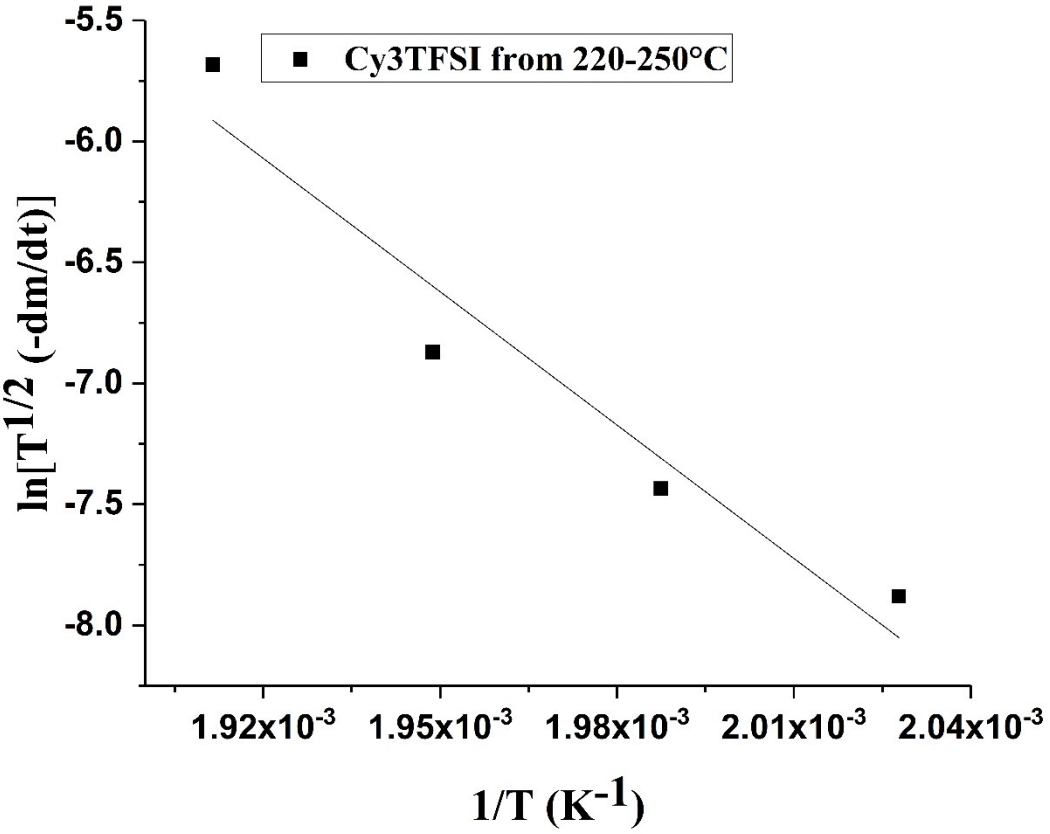

Figure S9. Plot of $ln[T^{1/2}$ (-dm/dt)] vs. T^{-1} to extract the slope for enthalpy of vaporization calculation.

Equation used to calculate the enthalpy of vaporization at average temperature (220-250°C):

$$\Delta_1^g H_m^\circ(T_{av}) = R\, S_L$$

R: universal gas constant 8.314 (J mol^{-1} K^{-1}), S_L: slope of ln[$T^{1/2}$ (-dm/dt)] vs. T^{-1} (K^{-1}).

Crystal Structures

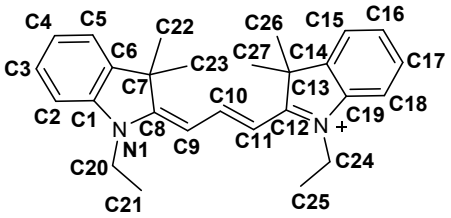

Figure S10. Cyanine atom numbering.

All crystal structures solutions and refinements were performed with common crystallographic software.[2,3]

The cyanines were numbered according to the cif file.

Overview about possible ways to access parameters describing anion-cation interactions in a single crystal

Since the anions and cations are complex molecules built from several atoms the term cation/anion radii needs further specifications and assumptions. Additionally the positive and negative charges are delocalised over several atoms. Therefore the coordination distance determination between the cation and anion is not a trivial task.

One disadvantage of commonly used methods is that the ions are treated as spherical objects. This assumption causes strong deviations from real situation where the ions represent several covalent bound atoms of irregular shape.

A simple and reliable model was developed for complex molecular ions which translates the ionic radii into a molecular volume.[2] The molecular volume can be precisely calculated for any geometrical shape taking information from the X-Ray structural data.

$$\Delta U = |Z^+||Z^-|\nu\left(\frac{a}{V_m^{\frac{1}{3}}} + \beta\right)$$

ΔU = Lattice energy, $|Z^+||Z^-|$ = charge of cation/anion, ν = number of ions per molecule, V_m = molecular volume, a = slope of the regression line: 117.3 kJ mol^{-1} nm (molecular volume against lattice energy of literature known salts), β = intercept of the regression line: 51.9 kJ mol^{-1} (molecular volume against lattice energy of literature known salts).

Table S8. Lattice energy calculation for Cy3TFSI and Cy3I.

Parameters	Compound	
	Cy3TFSI	Cy3I
a/nm (°)	1.02584 (90)	1.59149 (90)
b/nm (°)	1.60405 (90)	2.06750 (95.735)
c/nm (°)	1.88625 (90)	1.54852 (90)
Z	4	8
I	1	1
V_m/nm^{-3}	0.77596	0.63372
E_L/kJ mol^{-1}	359.09	376.93

Formula used to calculate Electrostatic Coulomb interactions:

$$E_{Coulomb} = \frac{1}{4\pi\varepsilon\varepsilon_0} \cdot \frac{z^2e^2}{r}$$

Z = ionic charge, r = shortest contact distance between cation and anion, ε_0 = vacuum permittivity, ε = relative permitivity of the material.

Since the original formula of Coulomb assumes spherical anions and cations the shortest cation-anion contact distance variable leads to a strong deviation from real conditions in complex molecular organic ions. The cation-anion distance can be replaced by the molecular volume.

$$r = \left(\frac{V_m}{2I}\right)^{\frac{1}{3}}$$

This modification provides more realistic values for complex molecular ions.

Table S9. Coulomb energy calculation.

Parameters	**Compound**	
	Cy3TFSI	Cy3I
ε	2.96	2.96
ε_0/ F m^{-1}	8.854×10^{-12}	8.854×10^{-12}
z	1	1
e/C	1.602×10^{-19}	1.602×10^{-19}
r/nm	0.729	0.63
E_c/eV	0.67	0.77

Table S10. Anion influence on bond lengths (Å) of the chromophore polymethine chain. *Average of the difference between C-C bond lengths in the polymethine chain. The values for Cy3I are given for both chromophores of the asymmetric unit.

Atom	TFSI	I
N1-C1	1.423(6)	1.413(4)/1.419(4)
N1-C8	1.360(5)	1.344(4)/1.342(4)
C8-C9	1.385(3)	1.385(4)/1.388(4)
C9-C10	1.386(3)	1.385(4)/1.378(4)
C10-C11	1.394(3)	1.385(4)/1.392(5)
C11-C12	1.380(3)	1.373(4)/1.379(4)
C12-N2	1.351(3)	1.351(4)/1.352(4)
N2-C19	1.408(3)	1.387(4)/1.412(4)
BLA*	0.77	0.43/1.23

Table S11. Anion influence on bending of the chromophore skeleton and indolenium ring conformation measured with Mercury 3.8.

Atoms	TFSI	I
C11-C12-N2-C19	174.1(9)	178.8(3)/178.1(5)
C11-C12-C13-C14	175.2(1)	177.4(5)/175.6(9)
C1-N1-C8-C9	172.2(3)	177.1(4)/178.9(1)
C6-C7-C8-C9	177.6(7)	177.0(2)/179.7(6)
C8-C9-C10-C11	177.0(4)	176.4(4)/178.1(1)

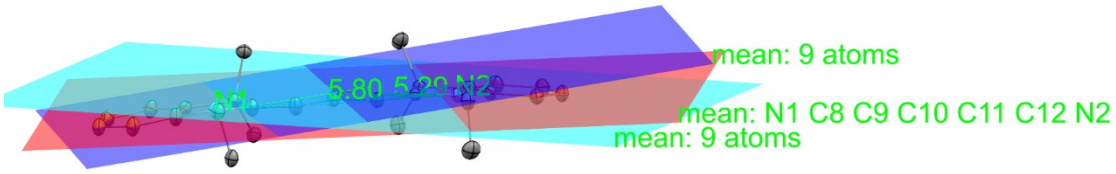

Figure S11. Chromophore bending angle measurement example.

With a low bond length alternation of 0.77 pm the Cy3TFSI polymethine chain polarisation lays in-between 0.43/1.23 pm observed for both chromophores of Cy3I. The delocalised π electron system is terminated by the two indolenium nitrogen atoms. Both chromophores are slightly concave bended with additional geometrical distortions of the indolenium rings with torsion angles obtained from C1/19-N1/2-C8/12-C9/11 and C6/14-C7/13-C8/12-C9/11 ranging between 174-177° for Cy3TFSI and 175-179° for Cy3I respectively.

Relative Permittivity

$\varepsilon_r = n^2 - k^2$

ε_r: relative permittivity (dielectric constant or function), n: real part of the index of refraction, k. imaginary part of the index (extinction coefficient)

The orientational polarization or dipole polarisation appears at low frequencies around 10^4 Hz. The n and k values are dependent on the wavelengths. At higher wavelengths however the slope is very low and at a certain wavelength the k value becomes 0.

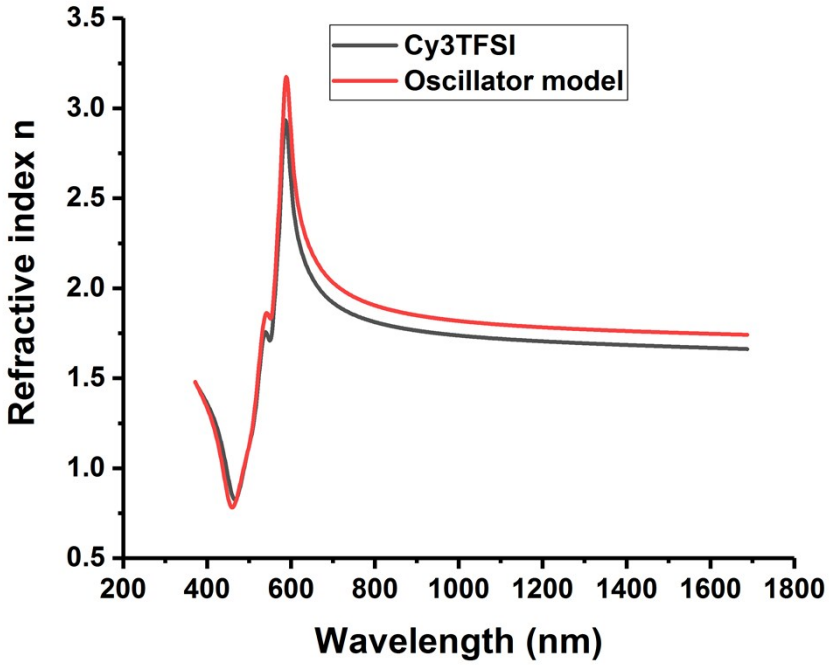

Figure S12. Function of n depending on the wavelength.

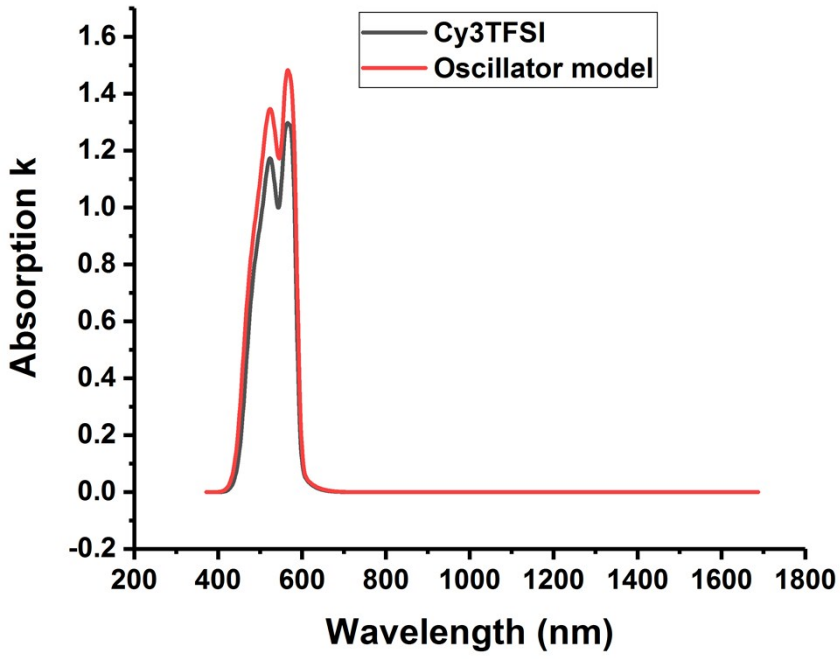

Figure S13. Function of k depending on the wavelength.

Therefore this area was chosen for the calculation of the dielectric constant. The n are given in this table as averaged values over the selected wavelength region.

Table S12. Calculated relative permittivity values for the Cy3TFSI.

Cyanine	n	λ/nm	ε_r
Cy3TFSI	1.72	823-1688	2.96

Thin Film Morphology

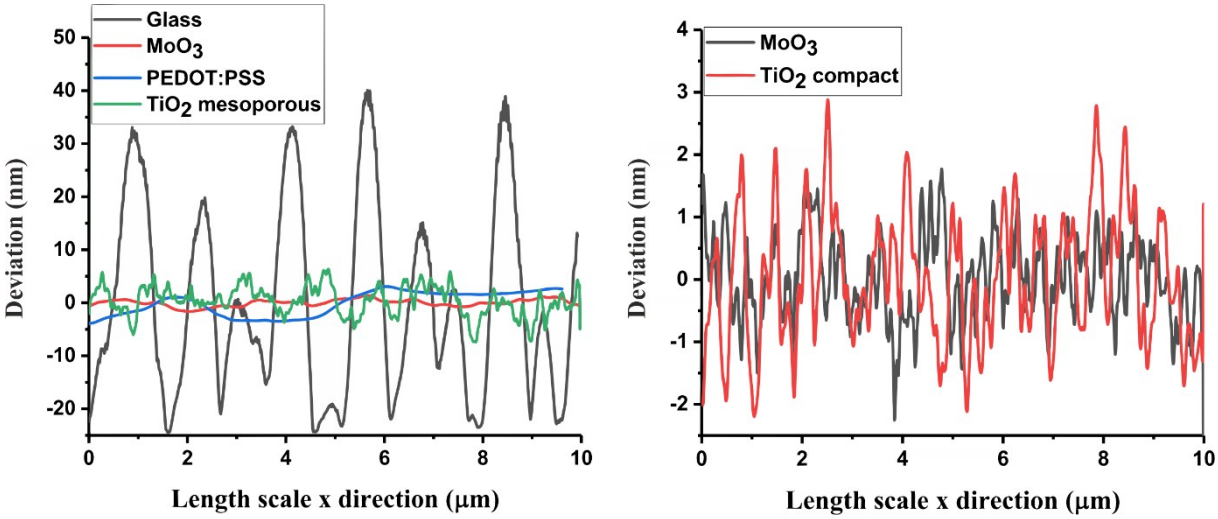

Figure S14. Roughness profiles obtained from different substrates of thin evaporated Cy3TFSI films.

Organic Photovoltaic Device Fabrication

Solution Spincast Bilayer Reference Device

As for usual cyanine organic photovoltaic devices, a bilayer stack was used with ITO/MoO_3(10 nm)/Cy3TFSI (10 nm)/C_{60} (40 nm)/Alq_3 (2 nm)/Ag (60 nm). The spincasting of the dye was performed under nitrogen atmosphere from TFP solution at 400 rpm for 60 s. After spincasting the substrate underwent a high vacuum treatment for 8 h at 6 × 10^{-6} mbar before the residual layers were evaporated. The statistics are presented in Table S13.

Table S13. Statistics of solution spincast Cy3TFSI cells

	N Cells	Mean	Standard Deviation	Min.	Median	Max.
V_{OC}/V	8	0.97	0.07	0.81	1.00	1.01
J_{SC}/mA cm^{-2}	8	4.67	0.26	4.40	4.62	5.12
Eff %	8	2.25	0.22	1.93	2.21	2.55
FF %	8	49.48	0.95	47.87	49.92	50.33

Solution Spincast Bulk Heterojunction Device

The trial to spin-cast Cy3TFSI and PCBM from chlorobenzene solution on a MoO_3 surface to form a bulk heterojunction morephology yielded phase separated dye/fullerene rich domains as illustrated in Figure S15.

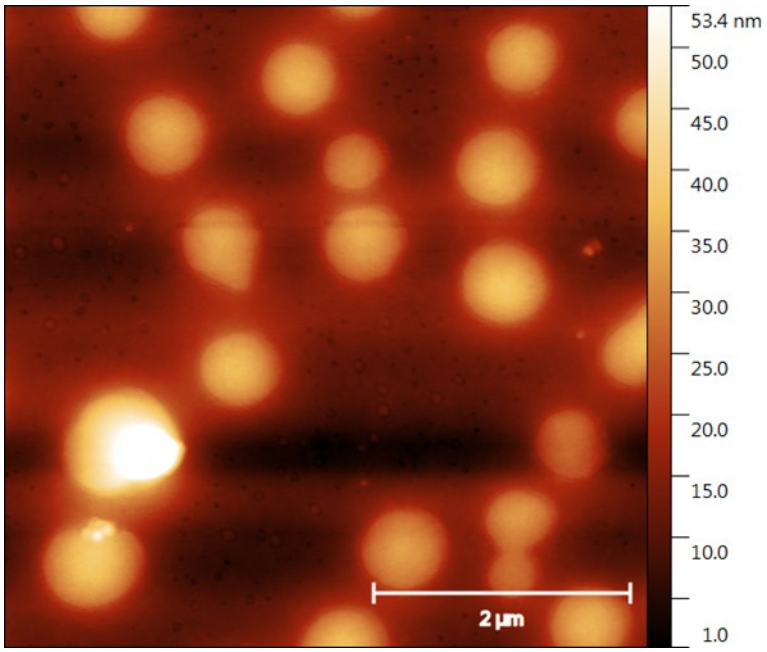

Figure S15. Morphology of spincast Cy3TFSI and PCBM blend.

As can be seen from Table S14, spincast bulk heterojunction devices showed only short circuited cells producing no valid statistical values.

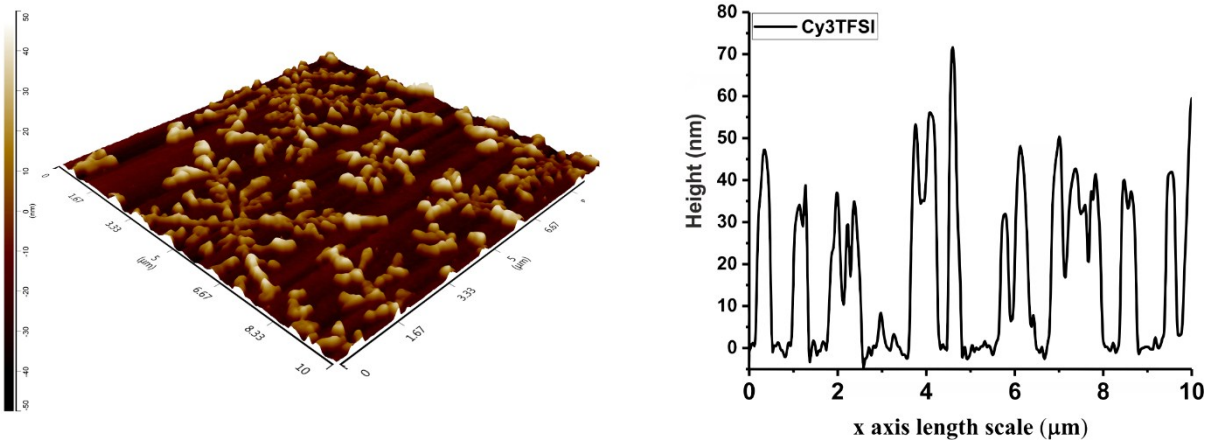

Figure S16. Topography of the coevaporated Cy3TFSI/C_{60} blend after 3 weeks storage in a glovebox.

Table S14. Statistical values of the short circuited Cy3TFSI/PCBM cells.

	N Cells	Mean	Standard Deviation	Min.	Median	Max.
Eff %	9	2.22E-4	1.54E-5	2.01E-4	2.21E-4	2.45E-4

Co-evaporated Bulk-Heterojunction Device

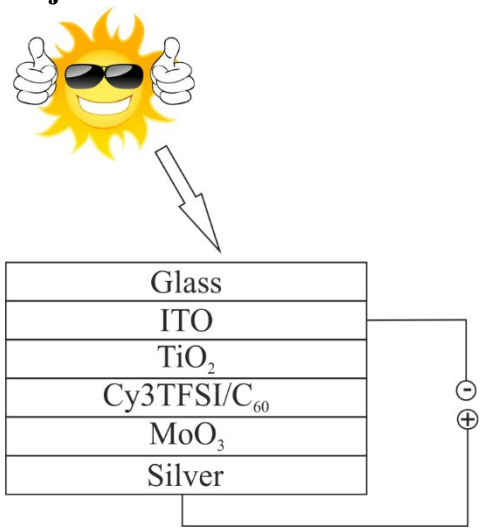

Figure S17. Architecture of the inverted bulkheterojunction cell.

The devices were made out of six layers: glass, indium tin oxide, TiO_2 (50 nm), Cy3TFSI/C_{60} active layer as co-evaporated bulkheterojunction (10 nm), molybdenum oxide (10 nm) as hole transport layer and silver (60 nm) as bottom electrode.

Table S15. Descriptive statistics of the measured Cy3TFSI cells.

	N	$\bar{x}_{arithm}$	s	Σ	min	$\bar{x}_{med}$	max
V_{OC}/V	19	0.63007	0.06067	11.97138	0.38763	0.64241	0.66975
J_{SC}/mA cm^{-2}	19	1.461	0.980	27.763	0.720	1.036	4.020
η	19	0.36075	0.24836	6.85428	0.15233	0.24708	0.9573
FF	19	38.98	2.41	740.55	30.91	39.48	41.52

Further Evaporated Device Stacks: First Trials

The following devices were fabricated without further optimizing the interlayer or active layer thicknesses.

Bulk heterojunction regular:

Glass/ITO/MoO_3/(Cy3TFSI/C_{60})BHJ co-evaporation/Alq_3/Ag (blue curve)

Bilayer inverted:

Glass/ITO/$TiO_{2\ compact}$/C_{60}/Cy3TFSI/MoO_3/Ag (green curve)

SSDSSC:

Glass/ITO/$TiO_{2\ mesoporous}$/Cy3TFSI/CuI/Ag (violet curve)

Bilayer regular:

Glass/ITO/PEDOT:PSS/Cy3TFSI/C_{60}/Alq_3/Ag (red curve)

Glass/ITO/MoO_3/Cy3TFSI/C_{60}/Alq_3/Ag (black curve)

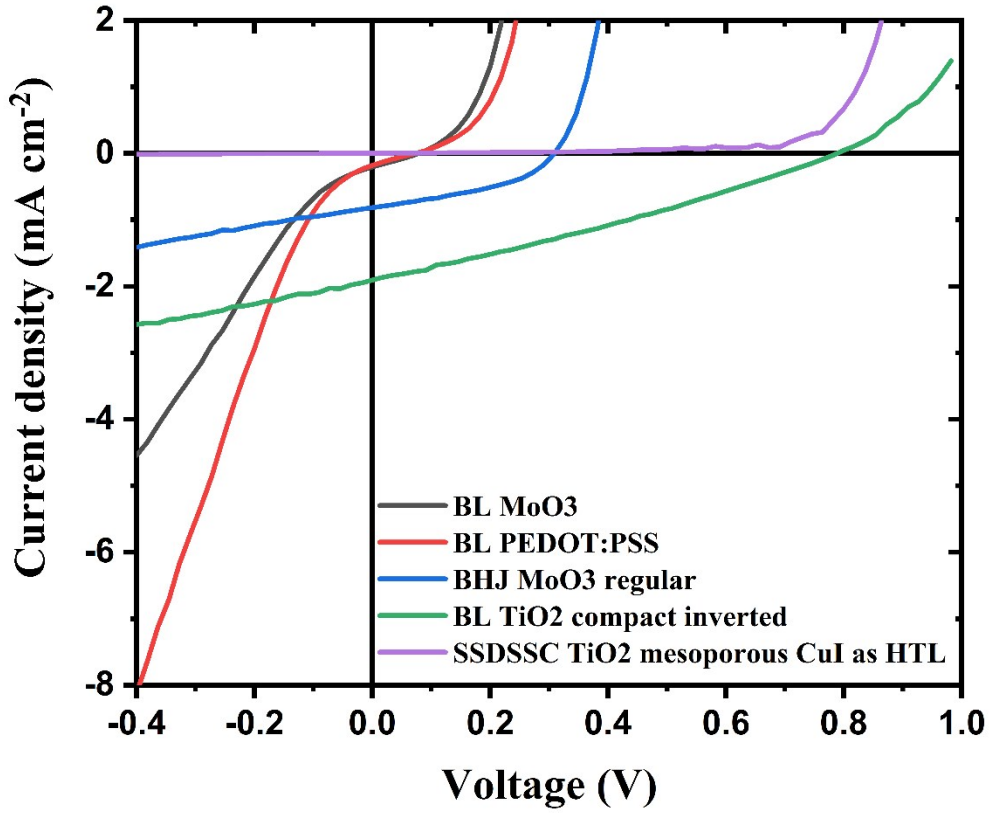

Figure S18. Summarized results from different device stacks of evaporated Cy3TFSI. The curves represent the cell response under illumination.

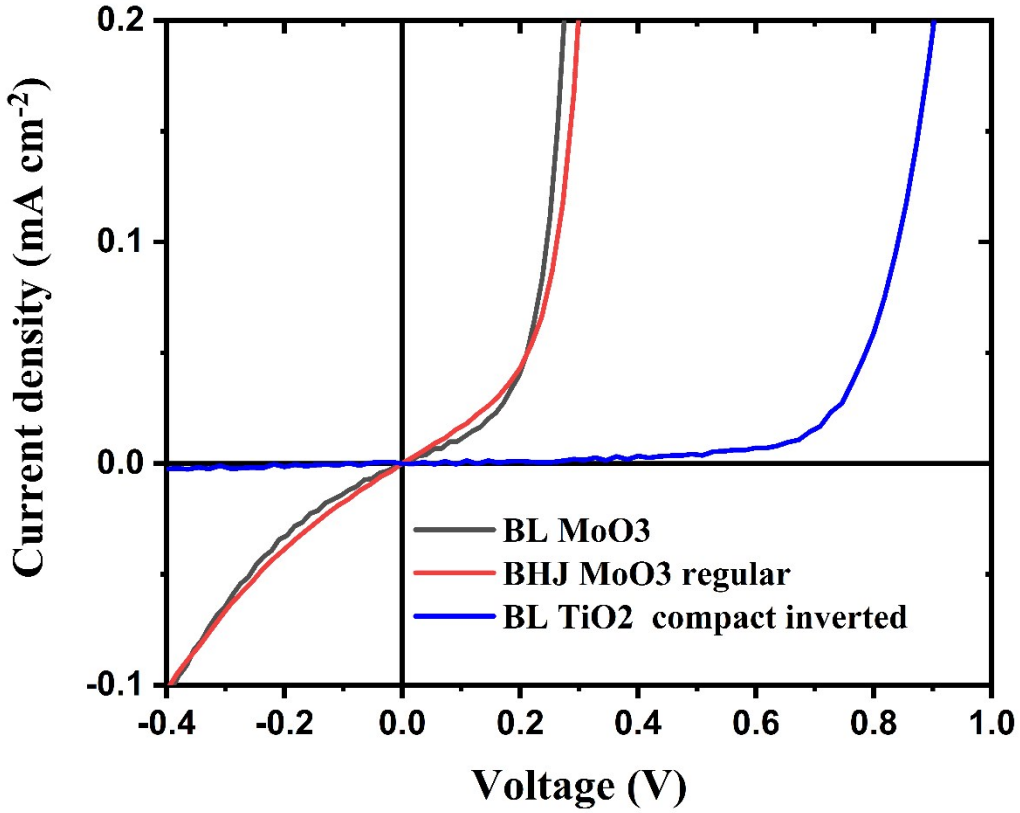

Figure S19. Dark current of the regular bulk heterojunction device, regular bilayer device geometry and of the inverted bilayer device geometry. Dark current of regular bilayer device with PEDOT:PSS as hole transport layer and SSDSSC devices were not measured due to the short lifetime of the cells.

Table S16. JV data of the representative evaporated Cells from Figure S17.

	V_{OC}/V	J_{SC}/mA cm^{-2}	η	*FF*
BL MoO_3	0.06	0.23	2.44x10^{-3}	17.07
BL PEDOT:PSS	0.06	0.24	1.4x10^{-3}	9.45
BHJ MoO_3 regular	0.30	1.12	0.10	45.11
BL TiO_2 compact inverted	0.77	1.89	0.42	29.01
SSDSSC TiO_2 mesoporous CuI as HTL	-0.05	-0.00	0	0

Sort Circuit Current Density Calculation

The short circuit current density $J_{sc} = \int EQE(\lambda)*\Phi_{AM1.5}(\lambda)*e\, d\lambda$ was obtained by integrating over $EQE(\lambda)$, the photon flux $\Phi_{AM1.5}(\lambda)$ of the AM1.5 solar spectrum and multiplying by the elementary charge e.

Literature

[1] [1] D. Gesevičius, A. Neels, S. Jenatsch, E. Hack, L. Viani, S. Athanasopoulos, F. Nüesch, J. Heier, *Adv. Sci.* **2018**, *5*, 1700496.

[2] H. D. B. Jenkins, H. K. Roobottom, J. Passmore, L. Glasser, *Inorg. Chem.* **1999**, *38*, 3609.
Sheldrick, G. M. (2008). Acta Cryst. A64, 112-122.

[3] Spek, A. L. (2003). J.Appl.Cryst. 36, 7-13.

[4] C. G. Zoski, *Handbook of electrochemistry*; Elsevier, 2007.

[5] J. L. Bredas, R. Silbey, D. S. Boudreaux, R. R. Chance, *J. Am. Chem. Soc.* **1983**, *105*, 6555.